



Herein, we investigate the host–guest complexation between cationic water soluble pillar[n]arenes (Fig. 1,  $n = 5$  and 6, **WP5** and **WP6**) and ribonucleotides (Fig. 1, AMP, ADP and ATP). Due to the differences in the cavity size of the hosts and the charge and length of the guests, **WP6** bearing six trimethylammonium groups on both sizes selectively complex with ATP. This host–guest recognition motif is employed to efficiently inhibit the hydrolysis of ATP in the presence of alkaline phosphatase (CIAP). This can be potentially utilized to overcome MDR. PEGylation by a hydrophilic diblock copolymer poly(ethylene glycol)<sub>142</sub>-block-(polyacrylic acid)<sub>22</sub> (Fig. 1, **FA-PEG-*b*-PAA**) endows the formed polyion complex (PIC) micelles with excellent targeting ability, preferentially delivering **WP6** to folate receptor over-expressing cancer cells. The ATP-dependent drug efflux pump was abated efficiently due to the inhibition of ATP hydrolysis by the formation of a stable host–guest inclusion complex **WP6**–ATP. As a consequence, the efficacy of cancer chemotherapy of doxorubicin hydrochloride (DOX·HCl) was significantly improved towards drug resistant human breast cancer cells (MCF-7/ADR) in the presence of **WP6**.

## Results and discussion

The host–guest complexations between the pillararene hosts (**WP5** and **WP6**) and guests (AMP, ADP and ATP) were first studied by <sup>1</sup>H NMR spectroscopy. Compared with the free guest (AMP, ADP or ATP), negligible chemical shift changes were observed for the protons on these ribonucleotide guests in the presence of **WP5** (Fig. 2b, S10 and S12<sup>†</sup>). The reason was that the cavity of **WP5** was too small to encapsulate the adenine group. On the other hand, almost no chemical shifts were observed for the protons on AMP (or ADP) in the presence of **WP6** (ESI, Fig. S14 and S16<sup>†</sup>) either, suggesting that the complexations between **WP6** and AMP and between **WP6** and ADP were not strong enough to include the adenine group into the cavity of **WP6**. However, the resonance peaks related to protons H<sub>a</sub>, H<sub>b</sub>, H<sub>d</sub>, H<sub>e</sub>, H<sub>f</sub> and H<sub>g</sub> of ATP disappeared, caused by a broadening effect after complexation upon addition of 1.0

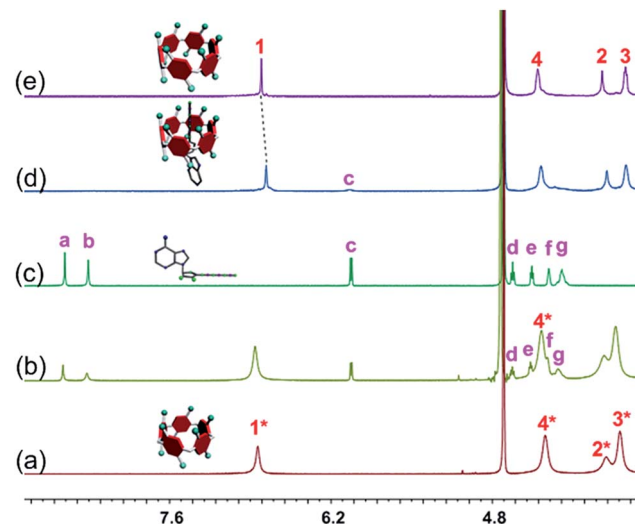


Fig. 2 Partial <sup>1</sup>H NMR spectra (400 MHz, D<sub>2</sub>O, 295 K): (a) **WP5** (1.00 mM); (b) **WP5** (1.00 mM) and ATP (1.00 mM); (c) ATP (1.00 mM); (d) **WP6** (1.00 mM) and ATP (1.00 mM); (e) **WP6** (1.00 mM).

equiv. of **WP6** (Fig. 2d). The reason was that these protons were located within the cavity of **WP6** and were shielded by the electron-rich cyclic structure by forming an inclusion complex between **WP6** and ATP.<sup>6c</sup> On the other hand, extensive broadening effect and upfield shifts were observed for the peak corresponding to proton H<sub>c</sub> due to complexation dynamics.<sup>14</sup> The results obtained from <sup>1</sup>H NMR spectra demonstrated that **WP6** could selectively complex with ATP, because the cavity size of **WP6** was suitable for ATP and the binding affinity was strong enough to form an inclusion host–guest complex mainly through electrostatic interactions and  $\pi$ – $\pi$  interactions between benzene rings and adenine.

<sup>31</sup>P NMR spectroscopy was also conducted to further verify the size-selective host–guest complexation between **WP6** and ATP (ESI, Fig. S11, S13, S15, S17 and S18<sup>†</sup>). No changes corresponding to the phosphorus signals of AMP (or ADP) were observed upon addition of **WP5** or **WP6** (3 equiv.). This was also true for the case of **WP5** and ATP. These phenomena were in

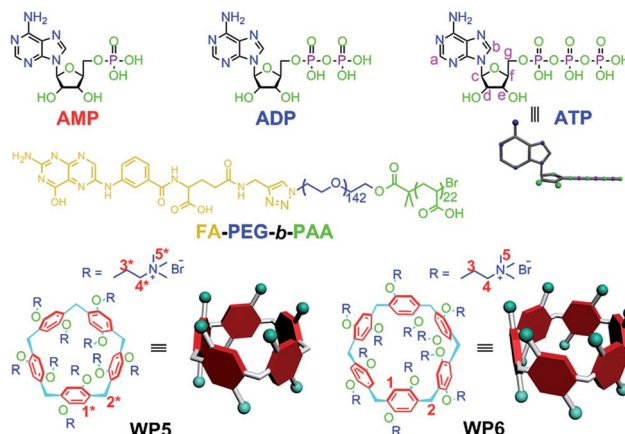


Fig. 1 Chemical structures of AMP, ADP, ATP, **WP5**, **WP6** and **FA-PEG-*b*-PAA**.

Table 1 Thermodynamic data, including association constants ( $K_a$ ), enthalpy changes ( $\Delta H$ ), and entropy changes ( $\Delta S$ ), obtained from ITC experiments for the complexes of **WP5** (or **WP6**) with the guests (AMP, ADP or ATP)<sup>a</sup>

Host	Guest	$10^{-3} K_a / M^{-1}$	$\Delta H / \text{kcal mol}^{-1}$	$\Delta S / \text{cal mol}^{-1} \text{K}^{-1}$
<b>WP5</b>	AMP	$2.78 \pm 0.35$	$85.9 \pm 6.7$	304
<b>WP5</b>	ADP	$3.92 \pm 0.43$	$64.3 \pm 5.1$	232
<b>WP5</b>	ATP	$26.2 \pm 3.30$	$8.99 \pm 0.76$	50.4
<b>WP6</b>	AMP	$2.86 \pm 0.23$	$42.8 \pm 2.2$	159
<b>WP6</b>	ADP	$4.38 \pm 0.43$	$16.9 \pm 1.4$	73.4
<b>WP6</b>	ATP	$152 \pm 16$	$4.58 \pm 0.42$	39.1

<sup>a</sup> Microcalorimetric titration experiments were conducted in PBS (pH = 7.4) at 298.15 K by titration of AMP (ADP or ATP) (2.00 mM, 10  $\mu$ L per injection) into the solution of **WP5** (or **WP6**) (0.100 mM).

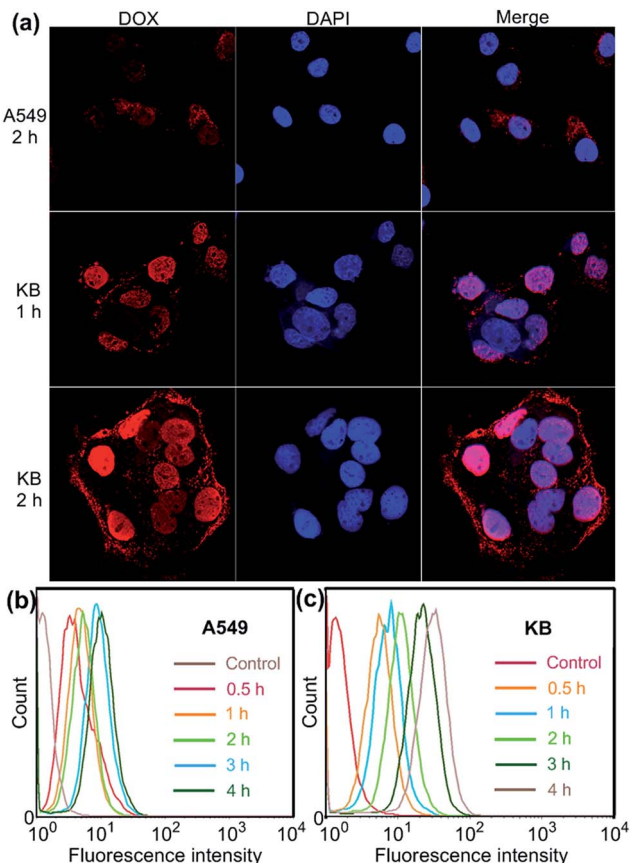


Fig. 3 (a) Confocal laser scanning microscopy (CLSM) images of A549 and KB cells incubated with DOX-HCl (5.00  $\mu\text{g mL}^{-1}$ ) loaded WP6/FA-PEG-b-PAA ternary PIC micelles. Flow cytometry showing increasing uptake of DOX-HCl (5.00  $\mu\text{g mL}^{-1}$ ) loaded WP6/FA-PEG-b-PAA ternary PIC micelles over a 4 h period using A549 (b) and KB (c) cells.

good agreement with the results obtained from  $^1\text{H}$  NMR studies (Fig. 2, S10, S12, S14 and S16 $\dagger$ ). On the contrary, the peaks related to the resonances of  $\alpha$ -ATP,  $\beta$ -ATP and  $\gamma$ -ATP all became broad and showed chemical shift changes upon addition of **WP6** (ESI, Fig. S18 $\dagger$ ), indicating successful complexation. A possible reason was that ATP was located in the cavity of **WP6** upon formation of an inclusion complex and shielded by its electron-rich cyclic structure.

Isothermal titration calorimetry (ITC) experiments were further performed to provide thermodynamic insight into the inclusion complexation between the pillar[n]arenes ( $n = 5, 6$ ) and ribonucleotides. As shown in Table 1, the enthalpy and entropy changes were obtained ( $\Delta H^\circ > 0$ ;  $T\Delta S^\circ > 0$ ;  $|\Delta H^\circ| < |T\Delta S^\circ|$ ), indicating that the complexations were driven by entropy changes. From comparison of the association constant ( $K_a$ ) values of these host-guest systems, we know that **WP6**  $\supset$  ATP exhibited the highest binding affinity, which further confirmed that **WP6** selectively complexed with ATP. Furthermore, NOE correlation signals were observed between proton H<sub>c</sub> on the ribose unit of ATP and proton H<sub>1</sub> on the benzene rings of **WP6** from the 2D NOESY NMR spectrum (ESI, Fig. S26 $\dagger$ ), indicating that ATP penetrated into the cavity of **WP6** to form

a [2]pseudorotaxane-type inclusion complex. Fig. S27 $\dagger$  shows the energy-minimized structure of **WP6**  $\supset$  ATP with the guest molecule tightly wrapped with **WP6**. Noticeably, the anionic segment of ATP locates on the upper side of **WP6** to successfully achieve multivalent electrostatic interactions with the cationic trimethylammonium groups. On the other hand, the repeating units of **WP6** rotate around the methylene bridges, changing its appearance from the pillar structure to a conical structure due to the asymmetric complexation.<sup>9b</sup> The ribose group threads into the cavity of **WP6** and it is surrounded by the benzene rings. Furthermore, the largest part (adenine group) of the ATP guest is situated at the relatively larger side of the conic **WP6**. The information obtained from molecular modeling is in good agreement with the NMR results mentioned above. Moreover, fluorescence titration experiments were carried out to provide evidence for the interactions between **WP6** and ATP. As shown in Fig. S25, $\dagger$  addition of ATP to a phosphate buffer solution of **WP6** resulted in a substantial decrease in the intensity of the emission band at 325 nm caused by host-guest complexation between **WP6** and ATP.

From the above discussions, we can know that the adenine group of the guest is included in the cavity of **WP6** for **WP6**  $\supset$  ATP while this group is not in the cavity of **WP6** for **WP6**  $\supset$  AMP and **WP6**  $\supset$  ADP. This should be ascribed to the differences in charge and length of these three guests. The length of the ATP is appropriate to maximize both multiple electrostatic interactions between the anionic segment of ATP and cationic ammonium units and  $\pi$ - $\pi$  interactions between benzene rings and the adenine group, as shown by the energy-minimized structure of **WP6**  $\supset$  ATP (ESI, Fig. S27 $\dagger$ ).

More interestingly, the hydrolysis of ATP was inhibited efficiently in the presence of **WP6**, in sharp comparison with the case of free ATP (ESI, Fig. S28–S30 $\dagger$ ). As indicated by  $^{31}\text{P}$  NMR spectra, the hydrolysis rate of ATP slowed down efficiently by forming a stable host-guest inclusion complex **WP6**  $\supset$  ATP in the presence of CIAP (6 U  $\text{mL}^{-1}$ ) (ESI, Fig. S30 $\dagger$ ). The reason was that ATP was located in the hydrophobic cavity of **WP6**, preventing ATP from being hydrolyzed.<sup>16</sup> The development of MDR to a variety of chemotherapeutic agents is one of the major challenges for efficient cancer treatment. One of the major causes of MDR is the over-expression of the drug efflux pump, the ATP-binding cassette superfamily membrane proteins, which transport anticancer drugs out of the cells and result in drug resistance by utilizing the energy from ATP hydrolysis.<sup>17</sup> Among various ATP-binding cassette superfamily membrane proteins, P-gp known as the ATP-dependent drug efflux pump which is upregulated in the plasma membrane of all MDR cancer cells, is probably the best characterized ABC transporter.<sup>18</sup> If the hydrolysis of ATP can be inhibited, the source of the chemical energy is cut off, resulting in the blocking of the efflux pump. On the other hand, the anticancer drugs can hardly be transported out of the cells through other energy-dependent approaches due to the shortage of energy, thus the efficacy of the cancer chemotherapy can be improved significantly.

In order to specifically block the cancer cells rather than normal cells, a folic acid functionalized hydrophilic diblock



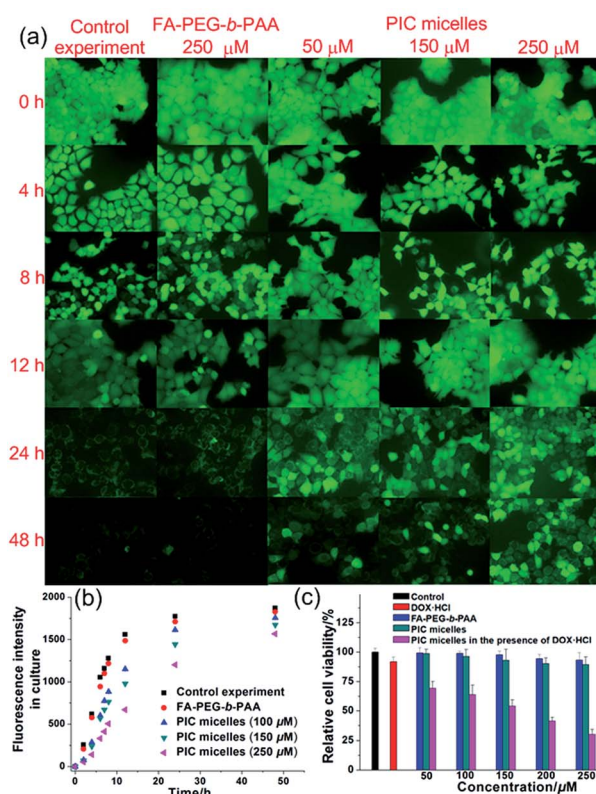


Fig. 4 (a) Fluorescence images of the MCF-7/ADR cells stained with calcein-AM incubated without/with FA-PEG-*b*-PAA (250  $\mu$ M), PIC micelles containing different amount of WP6.

(b) Fluorescence intensity changes of the culture in the presence of FA-PEG-*b*-PAA or PIC micelles containing different amounts of WP6.

(c) Cytotoxicity of DOX-HCl (25  $\mu$ M), FA-PEG-*b*-PAA, PIC micelles, and DOX-HCl (25  $\mu$ M) loaded PIC micelles with different concentrations of WP6 against MCF-7/ADR cells.

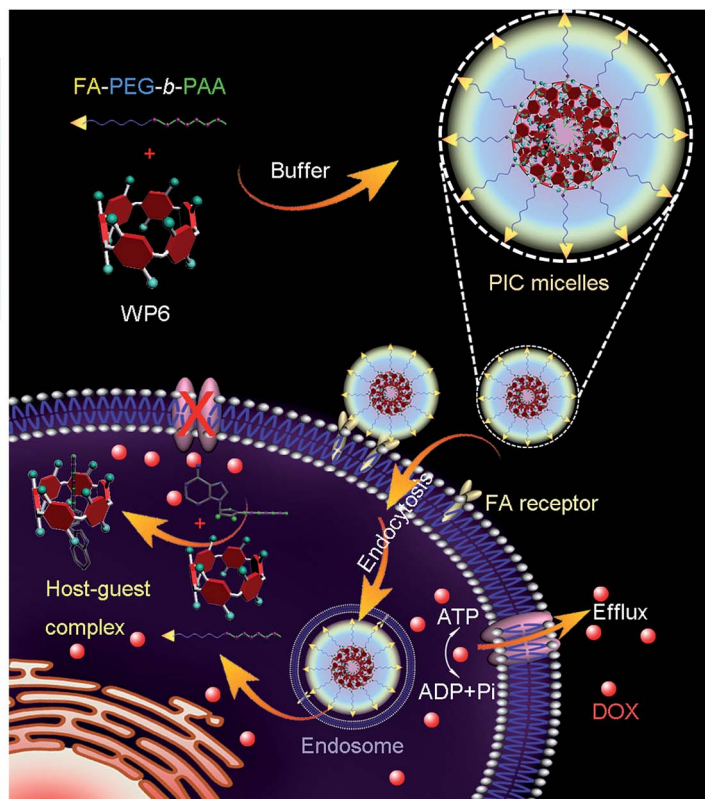


Fig. 4 (c) Cytotoxicity of DOX-HCl (25  $\mu$ M), FA-PEG-*b*-PAA, PIC micelles, and DOX-HCl (25  $\mu$ M) loaded PIC micelles with different concentrations of WP6 against MCF-7/ADR cells. Schematic illustration of the preparation of PIC micelles and possible mechanism to inhibit the efflux pump by forming a host–guest complex WP6 $\supset$ ATP in the cell.

copolymer **FA-PEG-*b*-PAA** was chosen to PEGylate the cationic **WP6**. Here **WP6** worked as a supramolecular cross-linker to interact with the negatively charged carboxylate segments of the diblock copolymer through electrostatic interactions in the buffer, forming stable polyion complex (PIC) micelles where **WP6** molecules and the anionic carboxylates are in the core of the PIC micelles, and the PEG blocks are on the surfaces of the micelles.<sup>19</sup> FA groups decorated on the surfaces of the PIC micelles endow these nanovehicles with the ability to specifically deliver **WP6** to folate receptor (FR) over-expressing cancer cells, because FR is a well-known tumor-associated receptor that is over-expressed in many tumors, including those of the breast, lung, kidney, and brain (*e.g.*, HeLa and KB cell lines), relative to normal tissue. On the other hand, PEGylation could also be employed to reduce the cytotoxicity of the cationic **WP6**.

In order to monitor the *in vitro* cell accumulation of the ternary PIC micelles as well as to confirm targeting delivery of these nanocarriers to FR over-expressing cancer cells, DOX-HCl as a commonly used anticancer drug with strong fluorescence was loaded into the PIC micelles formed by **FA-PEG-*b*-PAA** and **WP6**. TEM was employed to reveal the morphology of the ternary self-assembly formed by **FA-PEG-*b*-PAA**, **WP6** and DOX-HCl (charge ratio  $r = 1:1$ ). As shown in Fig. S31a,<sup>†</sup> spherical aggregates were observed with diameters ranging

from 100 to 170 nm, in good agreement with the results obtained from DLS (166 nm, ESI, Fig. S31b<sup>†</sup>). It should be emphasized that the DOX-HCl loaded ternary PIC micelles were quite stable in the buffer and showed no structural changes for several weeks.

Confocal laser scanning microscopic (CLSM) and flow cytometry investigations were conducted to verify whether the FA moieties decorated on the surface of the PIC micelles could guide these nanocarriers containing **WP6** preferentially to FR over-expressing KB cells, rather than FR low-expressing A549 cells. As shown in Fig. 3a, KB cells exhibited strong intracellular DOX-HCl fluorescence after incubation with DOX-HCl (5.00  $\mu$ g mL<sup>-1</sup>) loaded ternary PIC micelles for 1 h, and the fluorescence intensity became much stronger associated with extension of incubation time to 2 h. However, A549 cells showed weak fluorescence signal under the same experimental conditions (Fig. 3a). Moreover, red dots corresponding to the ternary PIC micelles affixed on the membrane of KB cells, indicating strong interactions between FA groups on the surfaces of the ternary PIC micelles and FRs on the cell membrane. Flow cytometry investigations demonstrated that KB cells always had faster uptake rate and higher intracellular accumulation than A549 cells (Fig. 3b and c). The mean fluorescence intensity was three times greater in KB cells than that in A549 cells ( $31.7 \pm 0.93$  vs.

10.6 ± 0.78) after incubation with the ternary PIC micelles for 4 h (ESI, Fig. S32†). These phenomena confirmed that the FA modified ternary PIC micelles could specifically enter the KB cells aided by the interaction of the FA moieties with FRs on the KB cells, possibly *via* receptor-mediated endocytosis.

Induced by the hydrophobicity, calcein acetoxymethyl ester (calcein-AM) can diffuse across the cell membranes, and be hydrolyzed to hydrophilic fluorescent calcein by esterase in the cytoplasm, so it can be employed as an excellent probe to test the operation of the efflux pumps in cell membranes by monitoring the fluorescence changes of the cell culture.<sup>20</sup> Fluorescence images provided visual colour changes of the cells stained with calcein in the presence and absence of **WP6** by culturing the cell for 48 h. As shown in Fig. 4a, the colour of the cells in the absence of **WP6** became weaker with the extension of culture time, indicating that calcein had a fast and profound release. In a parallel study by fluorescence microscopic observation, a similar phenomenon was observed for cells under the same incubation conditions in the presence of **FA-PEG-*b*-PAA**. While the fluorescence intensity of the cells changes much slower in the presence of **WP6** owing to the inhibition of ATP hydrolysis by forming **WP6**–ATP. Fig. 4b shows the release profile of calcein from the drug resistant MCF-7/ADR cells. Regardless of the presence of **WP6**, the release rate and the total release of calcein from cells were much higher than those in the presence of **WP6** by determining the fluorescence intensity of the cell culture. Accompanied with the enhancement of the concentration of **WP6** from 100 to 250 μM, the release rate and the total release of calcein from cells slowed down efficiently caused by the inhibition of ATP hydrolysis (Fig. 4b). The ATP-dependent calcein release underlined the significant role of **WP6** in the influence of the efflux pump by cutting off the energy source from ATP hydrolysis due to the formation of the host–guest inclusion complex.

The efficacy of the cancer chemotherapy of DOX·HCl in the presence and absence of **WP6** against MCF-7/ADR cell lines was carried out using 3-(4',5'-dimethylthiazol-2'-yl)-2,5-diphenyltetrazolium bromide (MTT) assay. As control experiments, the viabilities of MCF-7/ADR cells cultured with the diblock polymer **FA-PEG-*b*-PAA** or the PIC micelles were investigated, which showed minor cytotoxicity with concentrations ranging from 50 to 250 μM (Fig. 4c). On the other hand, the relative cell viability was 91.8% by culturing the cells with DOX·HCl (25 μM) (Fig. 4c). In stark contrast, the viability of MCF-7/ADR cells decreased from 69.2% to 30.3% accompanied with the increase of **WP6** from 50 to 250 μM in the presence of DOX·HCl at the same concentration (25 μM). The reason was that the source of the chemical energy was cut off by forming the stable inclusion complex **WP6**–ATP, resulting in the blocking of the efflux pump and other energy-dependent approaches to transport DOX·HCl out of cells. Therefore, the intracellular concentration of DOX·HCl was higher in the presence of **WP6** than those in the absence of **WP6**, resulting in the reduction of the corresponding relative cell viability, which indicated that the efficacy of the cancer chemotherapy DOX·HCl was improved significantly.

## Conclusions

In summary, a cationic water-soluble pillar[6]arene (**WP6**) selectively complexed with ATP to form a stable 1 : 1 inclusion complex **WP6**–ATP mainly driven by entropy change. As a result, the hydrolysis of ATP was efficiently inhibited in the presence of alkaline phosphatase due to the existence of a hydrophobic cavity of **WP6**. A folic acid ended diblock polymer **FA-PEG-*b*-PAA** was employed to PEGylate the cationic pillar[6] arene **WP6** to obtain PIC micelles in buffer, endowing them with specific targeting ability to deliver **WP6** to folate receptor over-expressing cancer cells. The ATP-dependent efflux pump was blocked by cutting off the energy source from ATP hydrolysis due to the formation of the host–guest inclusion complex. Furthermore, MTT assay demonstrated that the efficacy of the anticancer drug DOX·HCl was improved effectively in the presence of PIC micelles. The present results pave a way to develop novel therapeutic agents, implying that supramolecular chemistry may be engineered into promising vehicles to overcome multidrug resistance in cancer therapy. More detailed biologic investigations need to be carried out to figure out the deeper-level mechanism of the MDR treatment.

## Acknowledgements

This work was supported by National Basic Research Program (2013CB834502), the National Natural Science Foundation of China (21434005, 91527301), the Fundamental Research Funds for the Central Universities, the Key Science Technology Innovation Team of Zhejiang Province (2013TD02), and Open Project of State Key Laboratory of Supramolecular Structure and Materials (sklssm201611).

## Notes and references

- (a) M. I. Simon, M. P. Strathmann and N. Gautam, *Science*, 1991, **252**, 802; (b) A. Y. Ting, K. H. Kain, R. L. Klemke and R. Y. Tsien, *Proc. Natl. Acad. Sci. U. S. A.*, 2001, **98**, 15003.
- (a) S. M. Butterfield and M. L. Waters, *J. Am. Chem. Soc.*, 2003, **125**, 9580; (b) D. H. Lee, S. Y. Kim and J.-I. Hong, *Angew. Chem., Int. Ed.*, 2004, **43**, 4777; (c) M. B. Yaffe, *Nat. Rev. Mol. Cell Biol.*, 2002, **3**, 177; (d) S. K. Kim, D. H. Lee, J. I. Hong and J. Yoon, *Acc. Chem. Res.*, 2009, **42**, 23.
- (a) A. L. Davidson, *J. Bacteriol.*, 2002, **184**, 1225–1233; (b) C. F. Higgins and K. J. Linton, *Nat. Struct. Mol. Biol.*, 2004, **11**, 918–926; (c) M. F. Fromm, *Trends Pharmacol. Sci.*, 2004, **25**, 423–429.
- (a) A. P. de Silva, H. Q. N. Gunaratne, T. Gunnlaugsson, A. J. M. Huxley, C. P. McCoy, J. T. Rademacher and T. E. Rice, *Chem. Rev.*, 1997, **97**, 1515; (b) J. L. Sessler, V. Kral, T. V. Shishkanova and P. A. Gale, *Proc. Natl. Acad. Sci. U. S. A.*, 2002, **99**, 4848; (c) X. Zuo, S. Song, J. Zhang, D. Pan, L. Wang and C. Fan, *J. Am. Chem. Soc.*, 2007, **129**, 1042.
- (a) K. Kim, N. Selvapalam, Y. H. Ko, K. M. Park, D. Kim and J. Kim, *Chem. Soc. Rev.*, 2007, **36**, 267; (b) C. Schmuck, T. Rehm, K. Klein and F. Gröhn, *Angew. Chem., Int. Ed.*,



2007, **46**, 1693; (c) Z. Niu and H. W. Gibson, *Chem. Rev.*, 2009, **109**, 6024; (d) W. Jiang, A. Schäfer, P. C. Mohr and C. A. Schalley, *J. Am. Chem. Soc.*, 2010, **132**, 2309; (e) D.-S. Guo, K. Wang, Y.-X. Wang and Y. Liu, *J. Am. Chem. Soc.*, 2012, **134**, 10244; (f) K. Zhu, V. N. Vukotic and S. J. Loeb, *Angew. Chem., Int. Ed.*, 2012, **51**, 2168; (g) A. G. Campaña, D. A. Leigh and U. Lewandowska, *J. Am. Chem. Soc.*, 2013, **135**, 8639; (h) J.-F. Ayme, J. E. Beves, C. J. Campbell and D. A. Leigh, *Chem. Soc. Rev.*, 2013, **42**, 1700; (i) R. Barat, T. Legigan, I. Tranoy-Opalinski, B. Renoux, E. Péraudeau, J. Clarhaut, P. Poinot, A. E. Fernandes, V. Aucagne, D. A. Leigh and S. Papot, *Chem. Sci.*, 2015, **6**, 2608–2613.

6 (a) T. Ogoshi, S. Kanai, S. Fujinami, T. A. Yamagishi and Y. Nakamoto, *J. Am. Chem. Soc.*, 2008, **130**, 5022; (b) D. Cao, Y. Kou, J. Liang, Z. Chen, L. Wang and H. Meier, *Angew. Chem., Int. Ed.*, 2009, **48**, 9721; (c) M. Xue, Y. Yang, X. Chi, Z. Zhang and F. Huang, *Acc. Chem. Res.*, 2012, **45**, 1294; (d) H. Li, D.-X. Chen, Y.-L. Sun, Y. Zheng, L.-L. Tan, P. S. Weiss and Y.-W. Yang, *J. Am. Chem. Soc.*, 2013, **135**, 1570; (e) J. Fan, H. Deng, J. Li, X. Jia and C. Li, *Chem. Commun.*, 2013, **49**, 6343; (f) W. Si, Z.-T. Li and J.-L. Hou, *Angew. Chem., Int. Ed.*, 2014, **53**, 4578; (g) W.-B. Hu, H.-M. Yang, W.-J. Hu, M.-L. Ma, X.-L. Zhao, X.-Q. Mi, Y. A. Liu, J.-S. Li, B. Jiang and K. Wen, *Chem. Commun.*, 2014, **50**, 10460; (h) Z.-Y. Li, Y. Zhang, C. W. Zhang, L.-J. Chen, C. Wang, H. Tan, Y. Yu, X. Li and H.-B. Yang, *J. Am. Chem. Soc.*, 2014, **136**, 8577; (i) W.-B. Hu, W.-J. Hu, Y. A. Liu, J.-S. Li, B. Jiang and K. Wen, *Org. Lett.*, 2015, **17**, 2940; (j) X. Xiao, G. Nie, X. Zhang, D. Tian and H. Li, *Chem.-Eur. J.*, 2016, **22**, 941; (k) B. Yuan, J.-F. Xu, C.-L. Sun, H. Nicolas, M. Schonhoff, Q.-Z. Yang and X. Zhang, *ACS Appl. Mater. Interfaces*, 2016, **8**, 3679; (l) G. Yu, D. Wu, Y. Li, Z. Zhang, L. Shao, J. Zhou, Q. Hu, G. Tang and F. Huang, *Chem. Sci.*, 2016, DOI: 10.1039/C6SC00036C.

7 I. Nierengarten, S. Guerra, M. Holler, J.-F. Nierengarten and R. Deschenaux, *Chem. Commun.*, 2012, **48**, 8072.

8 Z. Zhang, G. Yu, C. Han, J. Liu, X. Ding, Y. Yu and F. Huang, *Org. Lett.*, 2011, **13**, 4818.

9 (a) N. L. Strutt, R. S. Forgan, J. M. Spruell, Y. Y. Botros and J. F. Stoddart, *J. Am. Chem. Soc.*, 2011, **133**, 5668; (b) G. Yu, Z. Zhang, C. Han, M. Xue, Q. Zhou and F. Huang, *Chem. Commun.*, 2012, **48**, 2958.

10 (a) Z. Zhang, Y. Luo, J. Chen, S. Dong, Y. Yu, Z. Ma and F. Huang, *Angew. Chem., Int. Ed.*, 2011, **50**, 1397; (b) C. Li, *Chem. Commun.*, 2014, **50**, 12420; (c) S. Wang, Y. Wang, Z. Chen, Y. Lin, L. Weng, K. Han, J. Li, X. Jia and C. Li, *Chem. Commun.*, 2015, **51**, 3434.

11 (a) H. Zhang, X. Ma, K. T. Nguyen and Y. Zhao, *ACS Nano*, 2013, **7**, 7853; (b) Q. Duan, Y. Cao, Y. Li, X.-Y. Hu, T. Xiao, C. Lin, Y. Pan and L. Wang, *J. Am. Chem. Soc.*, 2013, **135**, 10542; (c) Y. Cao, X.-Y. Hu, Y. Li, X. Zou, S. Xiong, C. Lin, Y.-Z. Shen and L. Wang, *J. Am. Chem. Soc.*, 2014, **136**, 10762; (d) G. Yu, W. Yu, Z. Mao, C. Gao and F. Huang, *Small*, 2015, **11**, 919.

12 N. L. Strutt, D. Fairen-Jimenez, J. Iehl, M. B. Lalonde, R. Q. Snurr, O. K. Farha, J. T. Hupp and J. F. Stoddart, *J. Am. Chem. Soc.*, 2012, **134**, 17436.

13 (a) G. Yu, Y. Ma, C. Han, Y. Yao, G. Tang, Z. Mao, C. Gao and F. Huang, *J. Am. Chem. Soc.*, 2013, **135**, 10310; (b) H. Chen, J. Fan, X. Hu, J. Ma, S. Wang, J. Li, Y. Yu, X. Jia and C. Li, *Chem. Sci.*, 2015, **6**, 197.

14 G. Yu, C. Han, Z. Zhang, J. Chen, X. Yan, B. Zheng, S. Liu and F. Huang, *J. Am. Chem. Soc.*, 2012, **134**, 8711.

15 (a) T. Ogoshi, H. Kayama, D. Yamafuji, T. Aoki and T.-a. Yamagishi, *Chem. Sci.*, 2012, **3**, 3221; (b) T. Ogoshi and T.-a. Yamagishi, *Eur. J. Org. Chem.*, 2013, 2961; (c) W. Chen, Y. Zhang, J. Li, X. Lou, Y. Yu, X. Jia and C. Li, *Chem. Commun.*, 2013, **49**, 7956; (d) N. Song and Y.-W. Yang, *Sci. China: Chem.*, 2014, **57**, 1185; (e) D. Xia, G. Yu, J. Li and F. Huang, *Chem. Commun.*, 2014, **50**, 3606; (f) J. Zhou, M. Chen and G. Diao, *Chem. Commun.*, 2014, **50**, 11954.

16 (a) G. Yu, J. Yang, D. Xia and Y. Yao, *RSC Adv.*, 2014, **4**, 18763; (b) B. Hua, J. Zhou and G. Yu, *Tetrahedron Lett.*, 2015, **56**, 986.

17 (a) M. M. Gottesman, T. Fojo and S. E. Bates, *Nat. Rev. Cancer*, 2002, **2**, 48; (b) G. Taubes, *Science*, 2008, **321**, 356; (c) N. Z. Kuhn and L. Nagahara, *Mol. Pharm.*, 2011, **8**, 1994; (d) I. Brigger, C. Dubernet and P. Couvreur, *Adv. Drug Delivery Rev.*, 2012, **64**, 24.

18 (a) M. Dean and T. Annilo, *Annu. Rev. Genomics Hum. Genet.*, 2005, **6**, 123; (b) P. D. Eckford and F. J. Sharom, *Chem. Rev.*, 2009, **109**, 2989.

19 (a) S. Fukushima, K. Miyata, N. Nishiyama, N. Kanayama, Y. Yamasaki and K. Kataoka, *J. Am. Chem. Soc.*, 2005, **127**, 2810; (b) C. Li, T. Wu, C. Hong, G. Zhang and S. Liu, *Angew. Chem., Int. Ed.*, 2012, **51**, 455.

20 Z. Mao, R. Cartier, A. Hohl, M. Farinacci, A. Dorhoi, T.-L. Nguyen, P. Mulvaney, J. Ralston, S. H. E. Kaufmann, H. Möhwald and D. Wang, *Nano Lett.*, 2011, **11**, 2153.